Opposed Flame Spread in Narrow Channel Apparatus to Assist in Suppression Studies

M. A. DELICHATSIOS[1], H. WANG[2], E. M. KENNEDY[2], B. MOGHTADERI[2], and B. Z. DLUGOGORSKI[2]
[1] FireSERT University of Ulster at Jordanstown
Newtownabbey, Co. Antrim
BT37 0QB, Northern Ireland, UK
[2] Process Safety and Environment Protection Research Group
Faculty of Engineering and Built Environment, The University of Newcastle
Callaghan, NSW 2308 Australia

ABSTRACT

In this paper, we study the performance of a testing apparatus that could be used for evaluating the effectiveness of gaseous suppressants and solid fuel retardants under opposed flame spread conditions. A narrow channel, 3 mm in height, 110 mm in width and 375 mm in length, constitutes the most important component of this apparatus. To establish the flow and flame spread parameters in this apparatus, thermally thick plates of a well characterized solid fuel, i.e., PMMA, were placed at the bottom of the channel whereas the top was a glass plate. A mixture of oxygen-enhanced air was introduced into the channel, and the fuel was ignited downstream to allow the flame to propagate in the direction opposite to the gas stream. The tests were recorded with a digital video camera and the rate of flame spread and the flame length were determined by analyzing the recorded images. The mass loss during an experiment was quantified by weighing a sample before and after each experiment. Extensive experimentation demonstrated that, the flame spread over the fuel in the channel is dominated by the velocity and oxygen content of the introduced gas stream, and a steady flame can be readily and reproducibly established. Simple theory and analysis provides correlations between the flame spread speed, the flame length and the mass of the material pyrolyzed during the flame spread by separating the thermal and flow from the chemical parameters. Thus, it is possible to investigate and assess the effectiveness of gaseous suppressants and solid fire retardants on reducing the flame spread and eventually leading to extinction.

KEYWORDS: flame spread, rate of flame spread, oxygen variation, suppression

INTRODUCTION

Understanding the behaviour and measuring the extinguishment concentration of gaseous fire suppressants are necessary for engineering design of fire-mitigation systems. From a fundamental perspective, the first step to attain this objective comprises an analysis of the behaviour of suppressants under idealised gas-phase conditions. Usually, these conditions are realised in laboratory-scale experiments of laminar pre-mixed flames, which involve measuring of laminar burning velocity followed by mechanistic calculations [1-5] In such calculations, it is convenient to evaluate the contribution of chemistry (reaction rates) and physics (thermal capacity and dilution) to the agent's effectiveness. Laminar diffusion flames, either in counter-current (opposed flow) or co-current (cup burner) geometries provide other experimental configurations to study the gas-phase extinguishment.

FIRE SAFETY SCIENCE–PROCEEDINGS OF THE EIGHTH INTERNATIONAL SYMPOSIUM, pp. 481-492

Until present, no methodologies have been developed to evaluate the performance of chemically active or inert gaseous suppressants for the extinguishment of fires of solid fuels. For example, currently, the design concentrations of gaseous suppressants against fires of solid fuels are obtained from the cup-burner experiments, which involve heptane as a liquid hydrocarbon fuel. This may be due to the fact that flames generated by solid fuels are often affected by a number of factors, including the physical and chemical properties of the solid which can be modified by fire retardants, spatial geometry of the fuel, flow field around the fuel and the presence of external energy sources. Furthermore, it is difficult to make detailed observations of the interaction between fire suppression agents and flames, as flames in an open space are considerably modified by natural convection. In addition, the burning of a solid is in general an unsteady process, with the combustion intensity often changing with time.

For the purpose of developing a test method for examining the behaviour of gaseous suppressants applied to fires of solid fuels, an attempt was made by the current authors to establish a stable flame over a solid fuel in a well-defined system [6]. The geometry of the system was based on the so-called Helle-Shaw cell, composed of two parallel thermally-resistant glass plates, placed close to each other to form a narrow channel. A specimen of solid fuel was located on the bottom plate and the distance between the top plate and the fuel was in the order of a few millimetres. Gas flow with a pre-defined concentration of oxygen was introduced into the channel from one end at the rate of a few litres per minute. The fuel was ignited downstream of the incoming flow to produce the so-called creeping (counter-current or opposed-flow) flame spread. This system can be also used to establish the effectiveness of fire retardant additives regarding the modification of the flame spread and extinction properties of a solid.

Preliminary experiments with a thin cardboard material indicated that the flame was easily established and moved forward along the fuel surface at a steady rate, when the flow-rate of the incoming flow was set within a reasonable range. The flame propagation velocity in the channel was controlled by the rate of the induced gas flow and its composition. Fire suppression agents added to the gas stream affected the chemical reactions occurring in the flame zone. However, the previous work has also demonstrated three drawbacks of using thin samples of cardboard material: (i) Such fuels are not thermally thick, making it difficult to simplify the energy equation that describes the flame spread.(ii) Large internal surface area and hygroscopic nature of dried cardboard specimens lead to uncontrollable absorption of moisture, even during short time periods necessary for mounting specimens in the experimental rig, after specimen removal from a desiccator and prior to commencement of the flow of nitrogen in a narrow channel. Preliminary experiments revealed that, the flame propagation velocity depends strongly on the moisture content at the cardboard surface, which in turn is a function of temperature and air humidity, with both of these parameters varying from day to day.

In the current work, efforts were made to characterize the operation of the existing system by introducing a new fuel type into the system, in the form of PMMA plates, 10 mm in thickness, to replace the thin cardboard material. The PMMA material, which has known physical and chemical properties, has been widely used in studies of flame spread over solid fuels. The plate introduced in the current system is thick enough to behave as thermally thick. The characteristics of flame spread over PMMA plates in the channel are then studied by extensive experimentation through variations of the flow rate and oxygen concentration of the incoming gas stream.

EXPERIMENTAL SETUP

A schematic diagram of the experimental setup is shown in Fig. 1. The apparatus consists of gas lines, narrow channel, and image recording system. Gases are introduced into the manifold from two compressed gas cylinders, which contain an O_2/N_2 mixture or O_2 and N_2 gases, separately. Using a pair of mass flow controllers, the concentration of oxygen and the flow rate of the gas stream can be set to any level. Oxygen concentration in the gas stream can be measured using an oxygen analyser (ADC 7000). Fire suppression agents can be added into the main stream at a pre-set flow rate. The gas stream is introduced into the narrow channel by a gas diffuser placed at the inlet of the narrow channel. The diffuser was designed to distribute the gas stream uniformly across the cross-sectional area of the channel.

Fuel samples, 10 mm thickness, are placed on an aluminium support. Placing a transparent fire-resistant glass plate on two aluminium spacers, separating the glass from the fuel, constitutes the channel. The distance between the fuel surface and the glass is always kept at 3 mm. Scale marks were etched on the bottom side of the top glass plate in increments of 10 mm. As the fuel and glass are very close to each other, the marks provide a reference for recording the flame spread over the sample. The narrow channel is 110 mm in width and 375 mm in length. A straight nichrome wire, powered through a low voltage transformer, is used to generate a linear flame on the sample surface just upstream of the channel exhaust. A digital video camera (DCR-TRV30E, Sony) serves to record the propagating flames in each experiment. A small canopy duct (not shown in Fig. 1) was used to vent the soot and smoke emerging from the channel exhaust.

Polymethyl-methacrylate, i.e., PMMA, was selected as the fuel in the current study. A local plastic supplier provided the material. The dark grey coloured pieces of PMMA (density 1.18 g/cm^3), supplied in 10 mm thickness, were cut into the rectangular shape, 364 mm in length and of 120 mm in width. The samples were dried in the well-sealed container, in the presence of silicon gel, for more than ten days and stored in the same container before use. The dried samples of PMMA had negligible moisture content because of their non-porous nature. The thermal properties of the PMMA material have been reported in the literature [7,8], with the melting temperature of between 220 and 240°C, the pyrolysis temperature of about 367°C, the specific heat of 2.2 kJ/(kg K) and the thermal conductivity of 0.282 W/(m K).

Prior to an experiment, a dried PMMA sample was weighed using an analytical balance (Mettler PM600) and then placed on the pre-shaped aluminium trough and held by two aluminium spacers at the sides. The glass plate and the aluminium spacers were held in place with a sealant. The entire channel assembly was clamped together to prevent leaks. The channel was then adjusted to the horizontal position using a spirit level. Gas mixtures of oxygen concentration of 49.8%, 79.8% and 100.0% by volume at standard conditions were introduced into the channel through the diffuser at predetermined flow rates between 1.96 and 7.32 L/min. Each experiment started by igniting the PMMA plate downstream at the exhaust end of the channel using the nichrome wire. As soon as the flame was well established and commenced to propagate uniformly along the surface of the PMMA plate, the digital video camera was started to record the spreading flames. Once the flame approached the diffuser by a distance of less than 10 mm, turning off the gas stream terminated the experiment. The sample was removed from the channel and weighed again, to determine the mass loss caused by the flame-spread process.

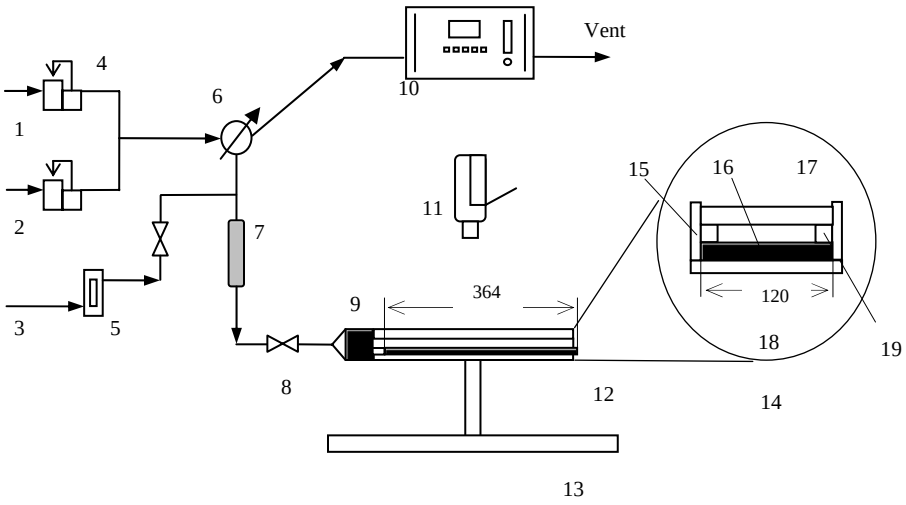

1 Gas line for nitrogen	6 Three-way valve	11 Digital video camera	15 Clip for the top plate
2 Gas line for oxygen	7 Drying tube	12 Narrow channel	16 Solid fuel
3 Gas line for fire agents	8 Gate valve	13 Stand for narrow channel	17 Top plate
4 Mass flow controller	9 Gas diffuser	14 Enlarged cross-section of narrow channel	18 Bottom
5 Rotameter	10 Oxygen analyser		19 Aluminium spacer

Fig. 1. Schematic diagram of the experimental apparatus.

By playing back the time–indexed images of flame spread recorded during each run, we extracted the location of the flame as a function of time. The average rate of flame spread was then determined from plots of distance versus time. The flame length was also measured from the recorded images of the flame. It was observed that steady flame spread was established.

EXPERIMENTAL RESULTS

A schematic diagram of flame spreading over the PMMA fuel in the narrow channel is illustrated in Fig. 2. The combustion reactions at the flame tip and in the flame zone generate a large amount of heat, with a portion transferred to the fuel by conduction and radiation. With a continuous heat penetration into the fuel, ahead of the flame, the PMMA polymer unzips (pyrolyses) into methyl methacrylate (MMA:$CH_3CH2CCOOCH_3$) monomer. Mixing of MMA fragments with the incoming oxidizer medium, in conjunction with the energy transfer from the existing flame tip, allows the fragments to ignite and the flame to move forward over the fuel surface [9]. Smoke, formed as a result of the combustion reactions in the flame zone, is transported downstream by forced convection with some smoke particles adhering on the bottom side of the top plate. The fuel surface after burning is fairly clean with only a small amount of char particles left on its surface.

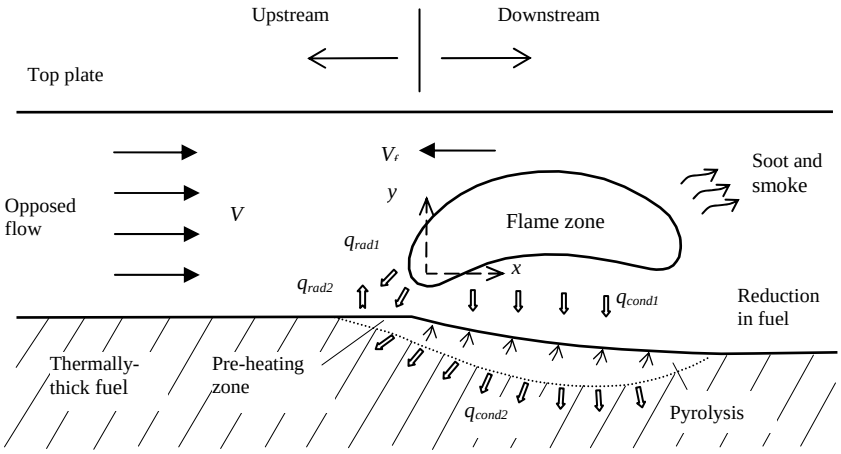

Fig. 2. Illustration of flame spread over a PMMA sample in the narrow channel.

Rates of flame spread for a number of upstream velocities and different oxygen concentration in the gas stream are shown in Fig. 3a. At a fixed oxygen concentration in the gas stream, the rate of flame spread increases monotonically with the gas velocity. The rate of flame spread is also sensitive to the oxygen concentration in the gas stream. For the same gas velocity, the rate of flame spread increases with increasing in the oxygen concentration in the gas stream. With an increase in the gas velocity, the flame length increases considerably, although the length of flame zone does not indicate a statistically significant dependence on the oxygen concentration; see Fig. 3b. The mass loss during the flame spread which evolved at a steady speed is shown in Fig. 4 to be influenced both by the gas velocity in the channel and by the oxygen concentration.

THEORETICAL ANALYSIS AND CORRELATIONS

Speed of Flame Spread

As seen in Fig. 2 and observed from the experiments, the leading edge of the flame at the solid surface spreads with a speed V_f against the opposed narrow channel flow, which has a gradient of the velocity near the wall of order equal to the average velocity in the channel, V_g, divided by the channel height H. The flame spread speed is steady and can be determined from an energy balance near the front that equates the convective energy, Q_c, needed to heat the solid fuel from the initial to its ignition temperature to the energy, E, given by the flame near the front [7,10,11]. The convective heat and the flame energy are determined next.

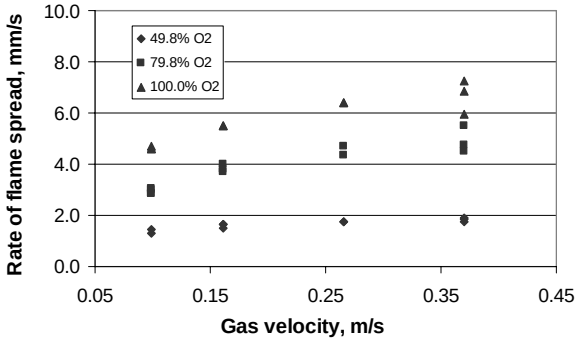

(a)

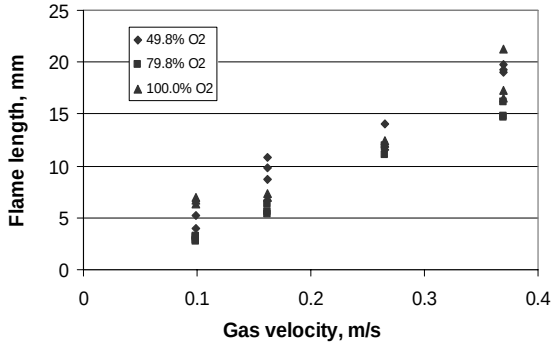

(b)

Fig. 3. Effect of the flowrate of the induced gas stream on the rate of flame spread (a) and the length of flame zone (b). Experiments were performed with mixtures containing 49.8, 79.8 and 100.0% of O_2.

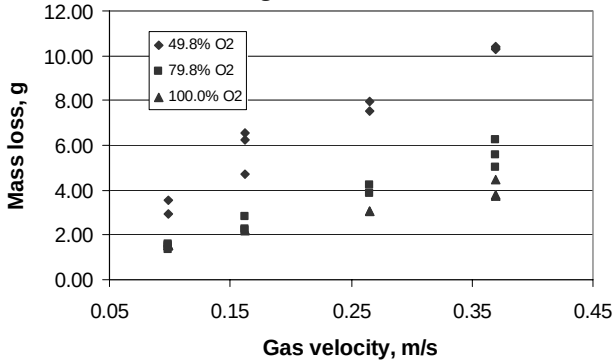

Fig. 4. Relationship between mass loss during flame spread and upstream gas velocity.

The convective heat to the solid (per unit width) is:

$$\text{Convective heat } Q_c = \rho_s c_s (T_{ign} - T_\infty) V_f \delta_s \quad (1)$$

Here ρ_s, c_s are the density and specific heat of the solid, T_{ign}, T_∞ are the ignition

and initial solid temperature and δ_s is the thermal depth in the solid during the heating of the solid by the flames near the front. This solid thermal depth is provided by simple diffusion theory as:

$$\delta_s \propto \sqrt{\alpha_s t_{res}} \tag{2}$$

Here, α_s is the thermal diffusivity of the solid and t_{res} is the residence time of the solid near the flame front which is equal to the effective gaseous thermal of the flame, δ_g, near the front divided by the speed of spread:

$$t_{res} = \frac{\delta_g}{V_f} \tag{3}$$

As discussed before the gradient of the flow near the front is proportional to V_g / H, so that by dimensional reasoning the gaseous thermal length is:

$$\delta_g \propto \sqrt{\alpha_g \frac{H}{V_g}} \tag{4}$$

with α_g being the thermal diffusivity in the gas phase.

By inserting Eqs. 2, 3, and 4 in Eq. 1 and rearranging, the convective heat becomes:

$$\text{Convective heat } Q_c = \rho_s c_s (T_{ign} - T_\infty) \sqrt{\alpha_s} \left[\frac{V_f}{\sqrt{V_g / H}} \right]^{1/2} \alpha_g^{1/4} \tag{5}$$

In Eq. 5 the first four quantities correspond to solid properties (which can be measured independently from other experiments such as the cone calorimeter), the last quantity to gaseous properties and the rest involve the flame speed and the gas velocity and height of the channel.

Returning now to the flame heat flux, it is straightforward [9,10] to observe that for infinitely fast kinetics this energy is :

$$E = k_g \frac{(T_f - T_{ign})}{\delta_g} \delta_g = k_g (T_f - T_{ign}) \tag{6}$$

with k_g and T_f being the conductivity of the gas and the (adiabatic) flame temperature at stoichiometric conditions, respectively. For finite kinetics, the energy from the flame will decrease as the Damkoler number (i.e., the ratio of flow to chemical time) near the front decreases [9,10].

The flame speed is found by equating Eq. 5 with Eq. 6:

$$\rho_s c_s (T_{ign} - T_\infty) \sqrt{\alpha_s} \left[\frac{V_f}{\sqrt{V_g / H}} \right]^{1/2} \alpha_g^{1/4} = k_g (T_f - T_{ign}) \tag{7}$$

In the present experiments, the solid fuel is fixed and the oxygen concentrations in the flow are high to ensure the kinetics are infinitely fast so that the energy flux from the flame will depend only on the flame temperature which increases with oxygen concentration. Therefore, Eq. 7 suggests to plot the flame speed data as $\frac{V_f}{\sqrt{V_g / H}}$ against the oxygen concentration as illustrated in Fig. 5. The correlation corroborates Eq. 7 (within the errors due to the experimental uncertainties) because all data collapse and the slope of the line is two since the temperature difference at the Right Hand Side of Eq. 7 is proportional to the oxygen mass fraction which for the present experiments is nearly equal to the volume fraction.

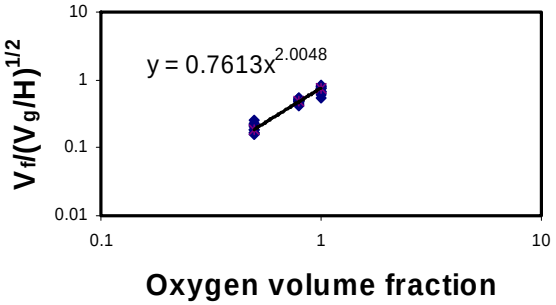

Fig. 5. Normalized flame spread velocity (incorporating the primary flow parameters, see Eq. 7) against oxygen volume fraction (nearly equal for the mass fraction here).

Flame Length

Gas concentration measurements at the exit and mass loss measurements show that the supply of air in the present experiments corresponds to globally under ventilated conditions. Thus the flame length can be determined by equating the flow of air into the flaming region with the entrainment in the boundary layer over the pyrolysing region up to the flame tip. This relation considers that all oxygen in the air is consumed because temperatures are high and reactions are fast in the present experiments. The mass flow of air supplied to the flames is equal to the mass flow in the channel (per unit width):

Supply of air: $\dot{m}_a = \rho_g V_g H$ (8)

Moreover the mass entrained by the flames is:

Entrained air by the flame $\propto \rho_g V_g \sqrt{\nu_g \frac{L_f}{V_g}}$ (9)

Here the term in the square root is the thickness of the boundary layer at the flame tip.

From the equality of Eqs. 8 and 9, the following expression for the flame height follows:

$$\frac{L_f}{H} \propto \frac{V_g H}{\nu_g} \tag{10}$$

The data of flame length in Fig. 3b and their independence on the oxygen concentration support Eq. 10 regarding their linear dependence on the flow velocity as shown in Fig. 3b. Equation 10 is not applicable if flame spread ceases or reaction rates are slow.

Mass Pyrolysis Rate

Dividing the total mass loss in Fig. 4 by the PMMA density, the total length and width (i.e., the channel width) of the pyrolysed region at the end of flame spread, the average depth of the material, δ_p , that has pyrolyzed can be determined. Using this depth and the steady flame speed, an average mass pyrolysis rate is:

$$\dot{m}_p = \rho_s \delta_p V_f \tag{11}$$

This mass loss is constant in time for the same experimental conditions because the flame speed and flame length remain constant and the local burning rate reaches a quasi-steady value owing to the high heat fluxes near the front. Guided by relations in under ventilated fires in enclosures, we formed the ratio of mass pyrolysis rate (in Eq. 11) over the air supply rate in the channel (in Eq. 8), and plotted it in Fig. 6. The results for the present geometry and flow show that this ratio is constant and equal to about 0.5 independent the gas flow velocity in the channel. To examine its dependence on oxygen concentration, the data in Fig. 6 are re-plotted in Fig. 7 with the abscissa being the oxygen mass fraction. Fig. 7 clearly shows that the ratio of mass pyrolysis rate over the gas supply rate depends on oxygen mass fraction. The behaviors in Figs. 6 and 7 are explained by the present theory in the following way. The depth of the pyrolysed material, δ_p, is proportional to the residence time of the material in the flames ($=L_f / V_f$) multiplied by the regression pyrolysis rate, which in turn is equal to the heat flux from the flame ($= k_g (T_f - T_{ign})/H$) divided by the heat of gasification ($=\Delta H_g$) and the density of the solid, ρ_s. Mathematically the pyrolysis depth is given by:

$$\delta_p = Residence time \; x \; Regr. rate \propto (\frac{L_f}{V_f})\{\frac{k_g (T_f - T_{ign})}{\rho_s H \Delta H_g}\} \tag{12}$$

After using Eq.10 and performing the algebra, Eq. 12 gives:

$$\frac{\dot{m}_p}{\dot{m}_a} = \frac{\rho_s \delta_p V_f}{\rho_g V_g H} \propto \frac{\alpha_g c_g (T_f - T_{ign})}{\nu_g \Delta H_g} \tag{13}$$

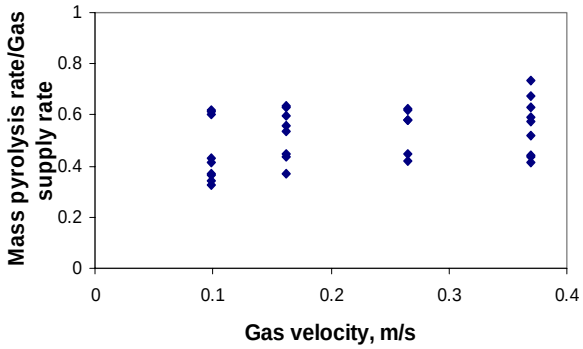

Fig. 6. Ratio of mass pyrolysis rate over the mass supply rate of gas plotted against the channel gas velocity.

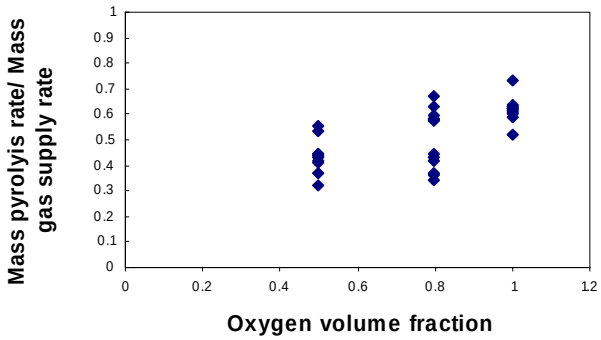

Fig. 7. Ratio of mass pyrolysis rate over the mass supply rate of gas plotted against the channel oxygen volume fraction (nearly equal to the oxygen mass fraction for the present values).

In the present experiments, the solid fuel is fixed and the oxygen concentrations in the flow are high enough to ensure the kinetics is infinitely fast so that the flame temperature increases proportional with the oxygen concentration. Therefore Eq. 13 is consistent with the experimental results in Figs. 6 and 7 because they confirm that the ratio of the mass pyrolysis rate to the mass supply rate of gas is independent of the gas velocity and varies almost linearly with the oxygen concentration (within the experimental errors). The latter behavior is consistent with the behaviour in Fig. 5 regarding the dependence of flame spread velocity on oxygen concentration.

Figures 3, 5, 6, and 7 can be the yardstick to evaluate the effectiveness in reducing or preventing flame spread of both gaseous suppression agents and fire retardants by measuring the deviations from these data. These deviations will be due only to chemical kinetics variations in the gaseous combustion because flow or thermal effects have been essentially separated. Measurements in the effluents in this apparatus can also determine toxic compounds.

CONCLUDING REMARKS

It was observed that flame propagates uniformly across thermally-thick plates of PMMA in a narrow channel apparatus shown in Fig. 1. The flame properties, i.e., the rate of flame spread, the length of the flame zone and the mass of pyrolsysed solid, are dependent on the velocity of the induced gas mixture and the oxygen concentration in the gas stream.

The rate of flame spread and the flame length measured during testing can be used as indices to rank the performance of gaseous agents and the effectiveness of fire retardants. This is possible because the effects of flow parameters have been separated from those of chemical kinetics based on a simple theory of flame spread and its validation by the present data, as expressed by Eqs. 7, 10, and 13 and Figs. 3, 5, 6, and 7.

Specifically, it has been shown in a mutually consistent fashion that:

- Flame length depends only on the gas velocity linearly (Fig. 3b and Eq. 10)
- Flame spread velocity correlates using a fundamental spread analysis (Fig. 5 and Eq. 7)
- The ratio of mass pyrolysis rate to the gas mass supply rate is independent of the gas velocity and varies almost linearly with the oxygen mass fraction (Fig. 7 and Eq. 13)

The narrow-channel apparatus is able to generate stable, slowly-moving flames propagating over surfaces of solid fuels while minimizing buoyancy influences. The apparatus provides a convenient setting to test the effectiveness of gaseous fire suppressants and fire retardants. Both inert and chemically active agents can be easily added into the gas stream, to be transported into the flame zone.

Furthermore, a gas chromatograph or a residual gas analyser can be set up to sample the composition of the exhaust gases, to determine the rates of formation of toxic combustion by-products in mitigated flames.

REFERENCES

[1] Simmons, R.F., “Fire Chemistry,” In: (G. Cox, ed.) Combustion Fundamentals of Fire, Academic Press, London, 1995, p. 405.

[2] Babushok, V., Noto, T., Burgess, D.R.F., Hamins, A., and Tsang, W., “Influence of CF_3I, CF_3Br, and CF_3H on the high-temperature combustion of methane,” *Combust. Flam*., **107**, pp. 351–367, (1996).

[3] Fallon, G.S., Chelliah, H.K., and Linteris, G.T., “Chemical Effects of CF_3H in Extinguishing Counterflow CO/air/H_2 Diffusion Flames,” Proc. 26th Symp. (Inter.) on Combust., Combust. Inst., 1996, p.1395.

[4] Bozzelli, J.W., Moghtaderi, B., Dlugogorski, B.Z., and Kennedy, E.M., “Inhibition Pathways in Brominated Halon-doped Methane Combustion,” CHEMECA’97, *Proc. 24th Australian and New Zealand Chem. Eng. Conf.*, Rotorua, New Zealand, September, 1997, SF4b: 1-5.

[5] Yuan, J., Misra, A., Leah Wells, L., Hawkins, S., Krishnan, A., Nathuji, R.B., Marshall, P., and Berry, R., "The Kinetics of Elementary Reactions of CF_3Br and CF_3I with H, OH, O and CH_3 radicals: Experiments, ab initio Calculations and Implications for Combustion Chemistry," *Proc. 4th Inter. Conf. on Chemical Kinetics*, NIST, Gaithersburg, MD, USA, July, 1997.

[6] Dlugogorski, B.Z., Wang, H., Kennedy, E.M., and Delichatsios, M.A., "Testing of Gaseous Fire Suppressants in Narrow Channel Apparatus," *Proc. An. Inter. Halon Options Tech. Working Conf.*, Albuquerque, May, 2002, NIST Special Publication 984, pp. 1-11.

[7] Chen, Y., and Delichatsios, M.A., "Creeping Flame Spread: Some New Results and Interpretation for Material Flammability Characterisation," Combust. Flame, **99**, pp. 601-609, (1994).

[8] West, J., Tang, L., Altenkirch, R.A., Bhattacharjee, S., Sacksteder, K., and Delichatsios, M.A., "Quiescent Flame Spread Over Thick Fuels in Microgravity," *Proc. 26th Symp. (Inter.) on Combust.*, Combust. Inst., 1996, pp. 1335.

[9] Fernandez-Pello, A.C., "The Solid Phase," In: (G. Cox, ed.) Combustion Fundamentals of Fire, Academic Press, London, 1995, p. 31.

[10] Delichatsios, M.A., "Creeping Flame Spread: Energy Balance and Application to Practical Materials," *Proc. of 26th Symp. (Inter.) on Combust.*, Combust. Inst., 1996, p.1495.

[11] de Ris, J.N., "Spread of a Laminar Diffusion Flame," *Proc. 12th Symp. (Inter.) on Combust.*, The Combust. Inst., 1969, p. 241.